Water Research 295 (2026) 125539

Contents lists available at ScienceDirect

Water Research

journal homepage: www.elsevier.com/locate/watres

Manganese removal in a full-scale constructed wetland for passive mine water treatment: Environmental factors and microbial communities

Charlotte Lafont [a,b], Stéphane Vaxelaire [b], Alexandre Gelabert [a], Catherine Joulian [b], Hugues Thouin [b,c], Frédéric Duré [b], Mickael Charron [b], Josselin Gorny [d], Delphine Vantelon [e], Fabienne Battaglia-Brunet [b,c], Éric D. van Hullebusch [a,*]

[a] Université Paris Cité, Institut de Physique du Globe de Paris, CNRS, 75005, Paris, France
[b] BRGM, Orléans, France
[c] CNRS, BRGM, ISTO, UMR 7327, Université d'Orléans, Orléans, France
[d] Autorité de sûreté nucléaire et de radioprotection (ASNR), PSE/ENV/SPDR/LT2S, F-92260, Fontenay-aux-Roses, France
[e] Synchrotron SOLEIL, L'Orme des Merisiers, Départementale 128, 91190 Saint-Aubin, France

HIGHLIGHTS

- Two distinct mechanisms control manganese removal during passive mine water treatment.
- Manganese carbonate precipitates and accumulates in wetland sediments under high alkalinity conditions.
- Mn oxidation occurs in the reed rhizosphere through mineral plaque formation.
- Potentially calcite-forming bacteria are present in water.
- Importance of surface area as a key design parameter.

GRAPHICAL ABSTRACT

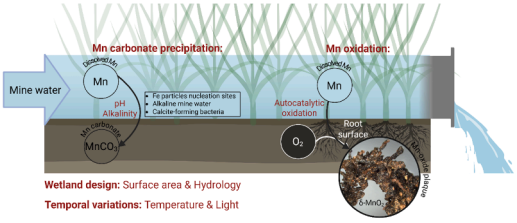

ARTICLE INFO

Keywords:
Manganese
Wetland
Mine water
Passive treatment
Iron
Microbial communities

ABSTRACT

Manganese (Mn) removal in passive mine water treatment remains a challenge due to its slow oxidation kinetics, requiring specific biogeochemical conditions. Constructed wetlands are often the key functional units enabling Mn removal in full-scale passive treatment plants. This study examines the key biogeochemical factors influencing Mn removal in a full-scale passive mine water treatment plant located in Alès (South-East France). Over one year, monitoring of physicochemical parameters, microbial communities, and Mn speciation in solid phases was conducted every two months. Results highlight temporal variations in Mn removal efficiency, with two main mechanisms identified: (1) Mn carbonate ($MnCO_3$) precipitation, likely influenced by high carbonate concentrations in mine water, and (2) Mn oxide (δ-MnO_2) formation, mainly associated with reed rhizosphere, where it accumulates as mineral plaque. In mine water, Mn removal correlates with Fe particle concentrations, suggesting a catalytic effect, as well as with alkalinity and the abundance of microorganisms affiliated to *Alteromonadaceae*, suggesting a microbial influence. Mn removal appears to be primarily abiotic, driven by favourable pH and alkaline conditions that promote Mn carbonate precipitation, by autocatalytic oxidation reactions occurring on rhizosphere surfaces and by plant's design including surface area and hydrological conditions. Microbial communities may facilitate certain Mn removal processes depending on environmental conditions.

* Corresponding author at: Institut de Physique du Globe de Paris, 1 rue Jussieu, 75238 Paris, France.
E-mail address: vanhullebusch@ipgp.fr (É.D. van Hullebusch).

https://doi.org/10.1016/j.watres.2026.125539
Received 14 November 2025; Received in revised form 27 January 2026; Accepted 8 February 2026
Available online 10 February 2026

1. Introduction

Mine water, also known as mine drainage water, poses a significant environmental challenge, as it often contains high concentrations of dissolved elements, including metals and metalloids (Ray and Dey, 2020). Its formation is typically due to rock-water interaction and oxidation of minerals like pyrite, although the pH can vary from acidic to alkaline depending on the buffering capacity of the surrounding minerals. While acidic mine water has been extensively studied due to its significant detrimental impact on ecosystems, circumneutral mine water also warrants attention due to its high concentration of potentially toxic and ecotoxic elements. Among the elements commonly found in mine water, manganese (Mn) and iron (Fe) are the most prevalent, with Mn posing a particular challenge in remediation systems (Neculita and Rosa, 2019). Elevated Mn levels raise concerns about water body contamination, as they can alter water taste, colour, and have harmful effects on ecosystems, including neurotoxic impacts on living organisms (World Health Organization, 2004).

Passive mine water treatment plants, such as constructed wetlands, provide an environmentally sustainable and cost-effective solution for long-term mine water remediation (Skousen et al., 2017; Younger and Wolkersdorfer, 2004). These systems rely on natural biogeochemical processes, including metal precipitation, sorption, sedimentation, and filtration, to remove contaminants. Compared to active treatment systems, passive plants require less energy and maintenance, making them economically attractive. However, these systems are subject to variations in environmental conditions, flow rate, and mine water chemistry over time, which can affect their efficiency. The design of effective passive systems is hindered by knowledge gaps related to the removal of dissolved metals, with Mn being particularly challenging due to slow abiotic oxidation kinetics (Younger et al., 2002). The high energy barrier for electron transfer from dissolved Mn to oxygen results in slow oxidation followed by precipitation (Morgan, 2005). Meeting discharge thresholds often requires extended hydraulic retention times, which in turn necessitate large surface areas (Younger et al., 2002).

Mn precipitation mechanisms are influenced by a range of factors that can enhance removal rates, including heterogeneous reactions catalysed by various mineral surfaces (Tebo et al., 2007). Additionally, various Mn-oxidising bacteria and fungi have been identified as key drivers of Mn removal kinetics (Diem and Stumm, 1984; Li et al., 2019). Moreover, while circumneutral pH conditions promote the oxidation of Mn, buffering compounds such as carbonates and bicarbonates can support the precipitation of Mn carbonate minerals, such as kutnahorite (Bamforth et al., 2006), and the presence of phosphorus promotes Mn-phosphate precipitation, such as metaswitzerite (Oliva et al., 2010).

Physicochemical conditions, such as pH, dissolved oxygen concentrations, temperature, dissolved Fe(II) concentrations, or concentrations of organic carbon or specific nutrients stimulating microbial activity, are affecting the rate of Mn removal (Lesley et al., 2008; Luan and Burgos, 2019; Moorhouse-Parry and Satterley, 2023). These key environmental parameters can shape the biogeochemical processes contributing to Mn removal by modifying the structure and activity of microbial communities, while in turn being regulated by microbial metabolisms (Faulwetter et al., 2009). Despite the identification of these parameters, the relationship between physicochemical parameters, microbial communities, and Mn removal efficiency in passive mine water treatment plants remains poorly understood.

While numerous studies have optimised Mn removal under laboratory-scale conditions, limited research has explored the optimal conditions for Mn removal in full-scale passive mine water treatment plants. This study aims to identify the mechanisms and factors influencing Mn removal in relation to temporal variations within the wetland treatment units. Over the course of one year, we monitored the chemical and physicochemical parameters of the mine water and analysed the composition of bacterial and fungal communities. In the final treatment unit, we further characterised sediment pore water, the mineralogical speciation of Mn and Fe, and the associated microbial communities to assess Mn removal mechanisms and the potential role of microbial communities. A deeper understanding of the biogeochemical processes governing Mn removal in passive treatment units can guide the design and operation strategies of these systems.

2. Materials and methods

2.1. Site description

The passive mine water treatment plant is located in Alès, France (44° 8' 49.1'' N, 4° 4' 18.6'' E, Fig. 1) and treats mine water from a former coal mine characterised by high Fe and Mn concentrations and high alkalinity content compared to typical natural surface water (Table 1). Mine water is pumped to the top of a six-step oxygenation cascade, with an average flow rate of 106 ± 3 $m^3 h^{-1}$ (data from April 2022 to February 2023, Table S1). The water then flows into a settling pond measuring 2 400 m^2 in surface area and 6 m in depth, followed by three consecutive aerobic planted wetlands of 1 540 m^2, 1 480 m^2 and 1 750 m^2 (Table S2). The wetlands are vegetated with reeds (*Phragmite* spp.) and exhibit variable water levels, ranging from 10 to 35 cm depending on sediment accumulation. Treated mine water is discharged into the Gardon River, with current discharge thresholds set at 2 mg L^{-1} for Fe and 1 mg L^{-1} for Mn, as specified by the regional prefectural decree. Monthly average precipitation at the site ranges from 0.68 to 3.98 mm day^{-1}, depending on the season. During the sampling period, rainfall occurred only during the December sampling campaign, with a total of 42.2 mm recorded (Figure S2).

Prior to this study, monitoring data reveal that the treatment plant exhibits wide variation in Mn removal efficiency (Figure S1), ranging from near complete to minimal removal. This variability offers valuable opportunities to investigate the factors influencing Mn removal. These preliminary data also indicate that Mn is mainly removed in the final wetland unit, while it is limited in the upstream units. The present study was therefore designed to examine the physicochemical and microbial factors that control Mn removal throughout the treatment units, with a particular focus on the processes occurring in the final wetland.

2.2. Water sampling

Water samples were collected from nine designated locations (Fig. 1) between April 2022 and February 2023 with a two-month sampling frequency. Sampling proceeded from the treatment plant outlet to the inlet using a conditioned sampling rod, with care taken to avoid sediment resuspension, as the sediments are easily disturbed. Each campaign was conducted over one or two days, and this duration may have influenced the observed data. In addition, between the June and the August sampling campaigns, the second wetland unit was mowed and left to cure as part of routine management. This event affected treatment performance and is considered a relevant variable in data interpretation. Samples were collected for the analysis of dissolved and total major and trace elements, dissolved carbon, Fe(II), anions, alkalinity and microbial community composition. Physicochemical parameters were acquired *in situ*. Details of on-site measurements and sample filtration, preparation and storage protocols are provided in the Supplementary Materials (Method S1).

2.3. Porewater characterization

During the sampling campaigns of December 2022 and February 2023, Diffusive Equilibrium in Thin-film (DET) probes were deployed to sample in situ pore waters and obtain concentration depth profile for Mn and Fe within the top 130 mm in the third wetland (Method S2). Probes were deployed at two locations: at the wetland entrance (S1, Fig. 1), with around 35 cm of sediment and no reeds, and at the middle point location (S2, Fig. 1), featuring dense reed growth and about 20 cm of

sediment.

2.4. Solid sampling

In March 2023, sediments and rhizomes were sampled from the third wetland, where most Mn removal occurs. This sampling represents a snapshot of Mn speciation rather than seasonal dynamics since temporal changes may alter Mn speciation but was limited to one campaign due to restricted XAS beamtime for solid analyses.

Sediment cores, corresponding to the upper 13 cm, were collected (Fig. 1, black squares) at the wetland's entrance (S1), middle (S2), and end (S3), targeting low reed-density areas to reduce rhizome and debris interference. Cores were obtained with 50 mL sterile syringes, sealed to maintain anoxic conditions, and subsampled in an N_2-purged glove bag into PP tubes. Rhizomes and associated mineral plaques were sampled near the outlet of the wetland using a shovel under a constant N_2 flush to limit exposure to O_2 (R, Fig. 1). Portions of rhizomes, untouched by the shovel, were stored in PP tubes under N_2. Samples were maintained under anoxic conditions using anaerocult® and divided in a glovebox into two portions: one stored at +4 °C for mineralogical characterisation and the other at -20 °C within 24 h for DNA extraction.

2.5. Chemical analyses

Elemental concentrations (*i.e.*, Al, As, Ca, Co, Fe, Na, K, Mg, Mn, Ni, P, S, and Zn) were measured by Inductively Coupled Plasma-Optical Emission Spectrometry (ICP-OES) using a SPECTROGREEN Spectro Analytical Instrument. Total acid digestion of solid samples was performed to determine major element concentrations by ICP-OES, following the protocol outlined in Method S3. Major anions (F^-, Cl^-, Br^-, NO_3^-, PO_4^{3-}, SO_4^{2-} and $S_2O_3^{2-}$) were analysed using an ionic chromatography system with DIONEX ICS1100. DOC and DIC were measured with a Shimadzu TOC-VCHS analyser. Water alkalinity was determined one day after sampling by titrating 10 mL of unfiltered water with 0.01 M HCl using a TitroLine® 7000 titrator (SI Analytics), and alkalinity values were calculated using the standard Gran method (Gran 1952). Water geochemical modelling was performed using PHREEQC software (Method S4).

2.6. Scanning Electron Microscopy (SEM) and energy dispersive X-ray analysis (EDX)

SEM observations were conducted on solid samples dried at room temperature within a glove box to preserve anoxia. Aliquots of dried sediment samples were then manipulated in the air to place them on carbon tape by sprinkling them with a spatula to preserve the elemental distribution within the sediment. This approach resulted in the formation of distinct sediment particle aggregates on the tape. Dried rhizome pieces displaying mineral plaques were directly placed onto the carbon tape. All samples were gold-coated and examined using a SEM AURIGA 40 (Zeiss) on the PARI platform. Imaging was performed at an acceleration voltage of 15 kV and a working distance of 15 mm. SEM-EDXS analyses were used qualitatively to confirm the presence of Mn in rhizosphere mineral plates and associated sediment particles, while Mn speciation was determined using XANES analyses.

Table 1
Physicochemical characteristics of influent mine water entering the treatment plant. Data accumulated during the monitoring period.

Parameters	Mean	SD
pH	6.5	± 0.1
ORP (mV)	-44	± 25
EC (µS.cm^{-1})	3970	± 260
Dissolved oxygen (mg.L^{-1})	0	± 0
Alkalinity (mM)	14.3	± 1.8
DOC (mg.L^{-1})	2.6	± 3.6
Ca* (mg.L^{-1})	503	± 90
Mg* (mg.L^{-1})	133	± 52
Fe* (mg.L^{-1})	28.4	± 6.5
Mn* (mg.L^{-1})	3.6	± 0.5

* Dissolved concentrations corresponding to < 0.45 µm filtered samples.

2.7. X-ray absorption spectroscopy (XANES)

XANES analyses at Mn and Fe K-edges were conducted on the LUCIA beamline at the SOLEIL synchrotron, France. Several sediment samples were dried under N_2 atmosphere and ground in an agate mortar to be prepared as a sample pellet. A piece of rhizome covered by mineral plaques was carefully pressed to form a pellet while maintaining the distribution of the mineral phases around the rhizome. Pellets were sealed in a holder with Kapton tape-covered and stored anoxically prior to being transferred to a sample mount at the beamline. The acquisition of XAS data, the list of standard samples, the processing methods, and the estimation of the fit are described in Supplementary Materials (Methods S5 and S6).

2.8. DNA extraction

DNA extractions from 0.22 µm Sterivex® filters were performed using the DNeasy® PowerWater® Sterivex™ Kit (Qiagen). For solid samples, DNA was extracted from approximately 0.5 g of wet material of

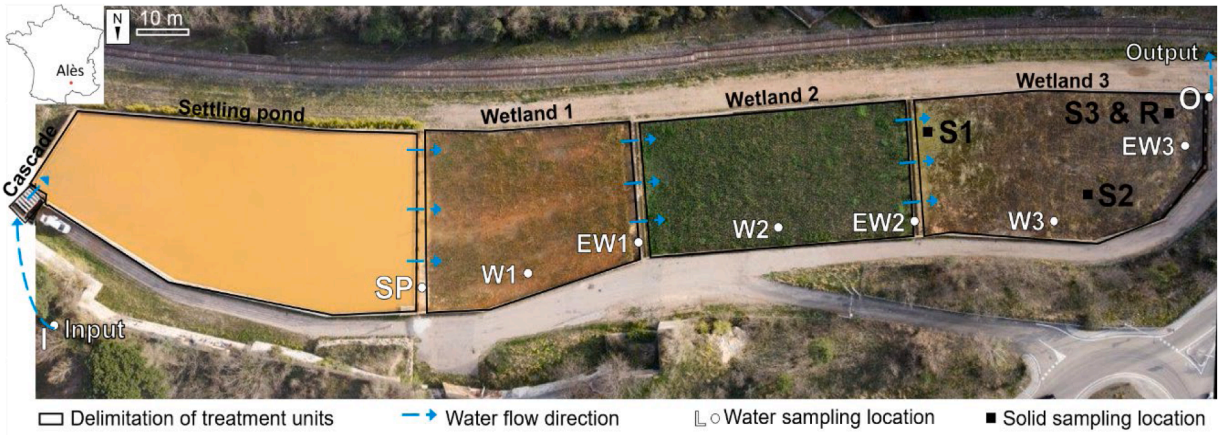

Fig. 1. Aerial photographs of the passive mine water treatment plant of Alès, showing the sampling points (white dots for water samples and black squares for sediments and rhizosphere samples) and the direction of the water flow path along the plant as shown by the blue arrows. SP = settling pond; W1-W3 = mid-sections of wetlands 1-3; EW1-EW3 = outlets of wetlands 1-3.

sediment and mineral plaques detached from the rhizome using the FastDNA® Spin Kit for Soil (MP Biomedicals). DNA quantification was carried out using the Promega Quantifluor® and the Quantus™ fluorometer. All extractions followed the protocols of the manufacturers. 16S rRNA and ITS sequencing and data processing are detailed in Supplementary Materials (Method S7). The raw datasets are available on the European Nucleotide Archive system under project accession numbers PRJEB107041 (16S data) and PRJEB107044 (ITS data).

2.9. Statistical analysis

All statistical analyses were performed using RStudio. Principal component analysis (PCA) was performed on the environmental data set, excluding sampling point I (Input, Fig. 1) due to its non-representative nature of the evolution of mine water composition and characteristics during passive mine water treatment. Pearson correlation analysis was performed to assess linear relationships among environmental variables. The Microeco package (version 4.2.3) was used for statistical analyses of the environmental factors and the microbial communities. Alpha-diversity indices were calculated (Chao1, ACE, Shannon, and InvSimpson index) to evaluate microbial richness and diversity of each sample. Beta-diversity analysis was performed to highlight dissimilarities among samples, and principal coordinate analysis (PCoA) of the Bray-Curtis distances matrix was calculated to visualise similarities of microbial communities between sample points throughout sampling campaigns. A multivariate analysis was performed using redundancy analysis (RDA) to elucidate the relationships between environmental variables and microbial communities during the passive treatment process.

3. Results and discussion

3.1. Spatial and temporal dynamics of Mn removal

The combined monitoring of the spatial and temporal physico-chemical characteristics of mine water contributes to a better understanding of the performance of the passive mine water treatment plant. Comparing the sampling locations, the dissolved Mn concentration gradually decreases from the inlet of the treatment plant, reaching its lowest value at the outlet (Fig. 2). No complete Mn removal was observed at any sampling month (43-92 %). The stable concentration of Mn between the settling pond and the second wetland is consistent with the slow removal rates of Mn observed under the physicochemical conditions prevailing in mine water (Lesley et al. 2008; Neculita and Rosa 2019). The pH, ORP, and DO reach high values by the wetlands (Figure S3), and an increase in Mn removal rates throughout the wetlands is observed (Table S3).

Across the six sampling campaigns, the Mn area-normalised removal rates were in the range of 0.5 to 1.1 g m^{-2} day^{-1} (Table S3). These values are consistent with previous studies which reported removal rates ranging from 0.1 g m^{-2} day^{-1} to 1.0 g m^{-2} day^{-1} in constructed wetlands (Bamforth and Satterley, 2022; Hedin et al., 1994). Lower values have been reported by Lesley et al. (2008) observing an Mn removal rate of 0.2 g m^{-2} day^{-1} despite a higher hydraulic retention time. The observed differences in Mn removal rates may be attributed to variations in mine water physico-chemical conditions, the use of different plant species, hydraulic conditions, or differences in the composition and activity of microbial communities. Here, the third wetland has the highest Mn area-normalised removal rates, ranging from 1.2 g m^{-2} day^{-1} to 3.0 g m^{-2} day^{-1} (Table S3).

Comparing the different sampling campaigns, Mn removal efficiency showed marked temporal variability. The highest Mn removal efficiencies were recorded in summer, reaching 88 % in June, while the lowest occurred in winter, with 32 % in December (Figure 2). In the third wetland, Mn removal efficiency fluctuated significantly: 43 % in April, 88 % in June, 57 % in August, 53 % in October, 32 % in December, and 61 % in February (Table S3). Sampling was carried out every two months, which limits the temporal resolution and prevents a complete assessment of seasonal dynamics, but the trends observed indicate consistent seasonal patterns.

The mine water flow remained relatively stable throughout the monitoring period (Table S1) (Luan and Burgos, 2019; Tum et al., 2024). However, several factors may account for the temporal variations in Mn removal rates, including (1) the direct effects of changes in physico-chemical parameters; (2) the indirectly influence of seasonal weather conditions on the physico-chemical parameters including temperature-dependent reactions; (3) the indirect effects of these parameters on the composition and activity of microbial communities; (4) the operational disturbances, such as the cured and mowed of the second wetland in early August (Section 2.2), which appears to have contributed to a decrease in Mn removal efficiency. These factors will be discussed in detail in the following sections.

3.2. Impact of iron on Mn removal

In passive mine water treatment systems, the initial treatment stages typically target Fe removal, as Fe is commonly present in mine water and readily oxidises and precipitates under oxygenated, non-acidic conditions (Hedin, 2008). The resulting iron-containing suspended particles are then removed through sedimentation and filtration (Wolkersdorfer, 2022). In this study, dissolved Fe concentrations are below the analytical detection limit (<35 µg L^{-1}) in the wetlands, and is

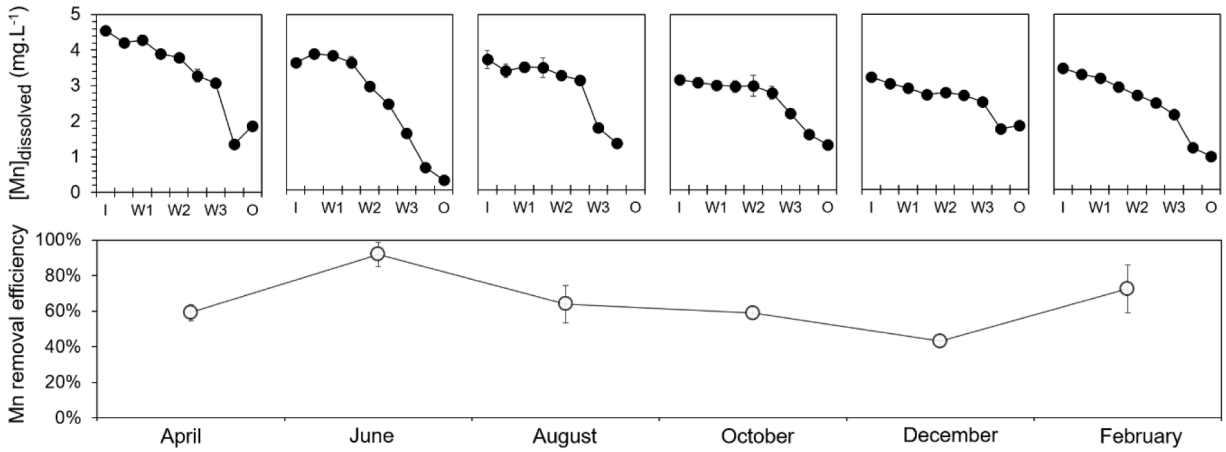

Fig. 2. Dissolved manganese concentration along the passive mine water treatment plant and manganese removal efficiencies of the plant for each sampling campaign. Sampling site locations are displayed in Fig. 1.

present as suspended particles in water, corresponding to the total Fe concentrations measured.

The total Fe concentration decreases alongside with the dissolved Mn concentration (Fig. 3), showing a positive correlation with R2 = 0.628 ($p < 0.01$, Figure S4). This relationship does not demonstrate a causal mechanism but may reflect similar spatial and temporal dynamics of Mn and Fe in the system. Such co-variation is probably the result of shared hydrological controls, including transport processes and physical disturbance, as observed after mowed and cued of the second wetland. On the other hand, Mn(II) oxidation can potentially occur on Fe oxide surfaces such as ferrihydrite, identified as the dominant mineral phase (Figure S5 and Table S4), but no direct evidence has been found (Davies and Morgan, 1989; Lan et al., 2021; Liu et al., 2022).

Moreover, Mn oxide is not the dominant phase identified in the sediment of the wetland, accounting for less than 10% of the total Mn content (Fig. 4 and Table 2). Instead, Mn carbonate is the primary detected Mn-bearing mineral, representing over 90% of Mn in samples S1 and S2 and 72.7 % in S3. The low proportion of Mn oxides may be attributed to system heterogeneity, suggesting that Mn speciation in sediment may not have been fully captured, or to competition with carbonate ions, which have favoured Mn carbonate precipitation over Mn oxide formation as supported by a positive saturation index of rhodochrosite in the water (Table S6). Although direct evidence of Fe particles contributing to Mn removal was not observed, their involvement remains plausible, as they could act as nucleation sites for carbonate precipitation (Schaefer et al., 2020; Zeng and Tice, 2014).

3.3. Alkalinity controlling Mn removal

The PCA (Fig. 3) and Pearson correlation matrix (Figure S4) reveal a strong positive correlation between alkalinity and dissolved Mn concentration ($r = 0.765$, $p < 0.001$). Mine water is characterised by high alkalinity and high Mn concentrations, the presence of rhodochrosite in all three sampling locations (S1, S2 and S3; Figs. 1 and 4). The water is saturated with rhodochrosite (Table S6) indicates that carbonate precipitation represents a primary pathway for Mn precipitation during

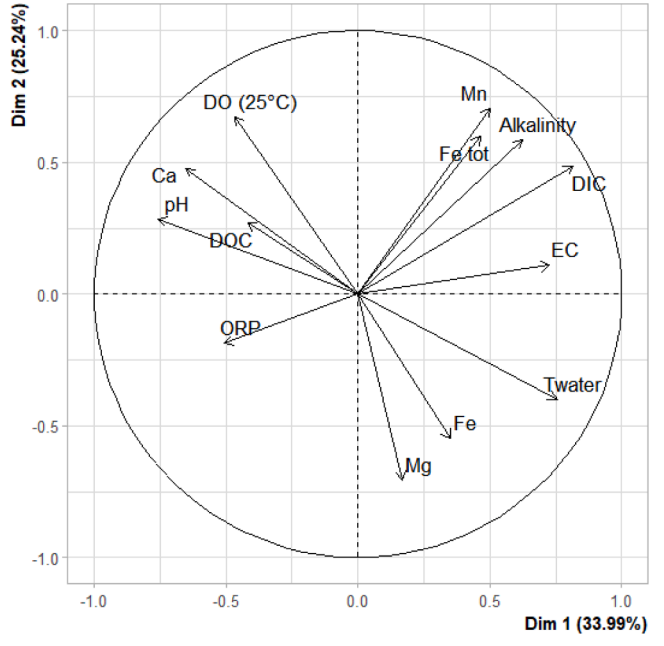

Fig. 3. Principal component analysis (PCA) of the physicochemical and chemical parameters, explaining 59.23 % of the total variance in the dataset. Data from the inlet sampling point (I) were excluded from the PCA due to their non-representativeness of the mine water composition evolution during the passive treatment process. Parameters included are Mn (dissolved Mn), Fe (dissolved Fe), Fe tot (total Fe), DIC (dissolved inorganic carbon), DOC (dissolved organic carbon), Ca (dissolved Ca), Mg (dissolved Mg), DO (25°C) (dissolved oxygen corrected to 25 °C), ORP (oxidoreduction potential), T_{water} (water temperature), pH, alkalinity, and EC (electrical conductivity).

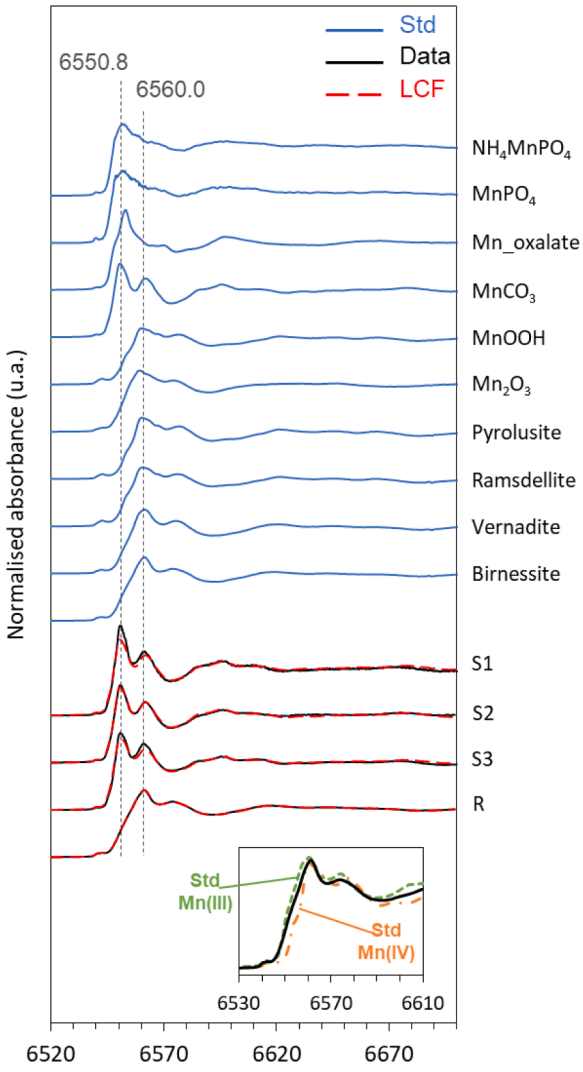

Fig. 4. Linear Combination Fitting (LCF) of XANES spectra at the Mn K-edge. Data include sediments S1, S2, and S3, and rhizosphere mineral plaque R from the third wetland. The black curve represents the sample spectra, and the red curve corresponds to the LCF fitting curve. A zoomed-in view of the R spectra highlights its intercalation between our Mn reference samples with a redox state of III (green) and a redox state of IV (orange). Linear Combination Fitting (LCF) results of Mn K-edge XANES spectra.

Table 2
Linear Combination Fitting (LCF) results of Mn K-edge XANES spectra.

Sample	% $NH_4Mn(II)PO_4$	% Mn (II) CO_3	% Mn $(III)_2O_3$	% d-Mn $(III/IV)O_2$	% Total	Chi^2_R	Rf
S1	6	93	0	0	99	2.04E-03	2.46E-03
S2	4	94	0	1	99	3.74E-04	4.46E-04
S3	20	73	0	8	101	8.88E-04	1.04E-03
R	7	0	10	83	100	3.19E-05	3.82E-05

mine water treatment (Bamforth et al., 2006; Kruse and Younger, 2009)

The Mn oxide content in sediment of the third wetland increases toward its outlet, as indicated by a shift in the XANES edge position and a slight rise in the contribution of the δ-MnO_2 reference spectrum to the XANES fit (Fig. 4). However, the Mn oxide contribution remains low compared to carbonate, below the detection limit of 10 % of the LCF in all the sediment samples (Table 2) and is in line with the saturation indices of Mn oxide (pyrolusite) which remain undersaturated in the water (Table S6).

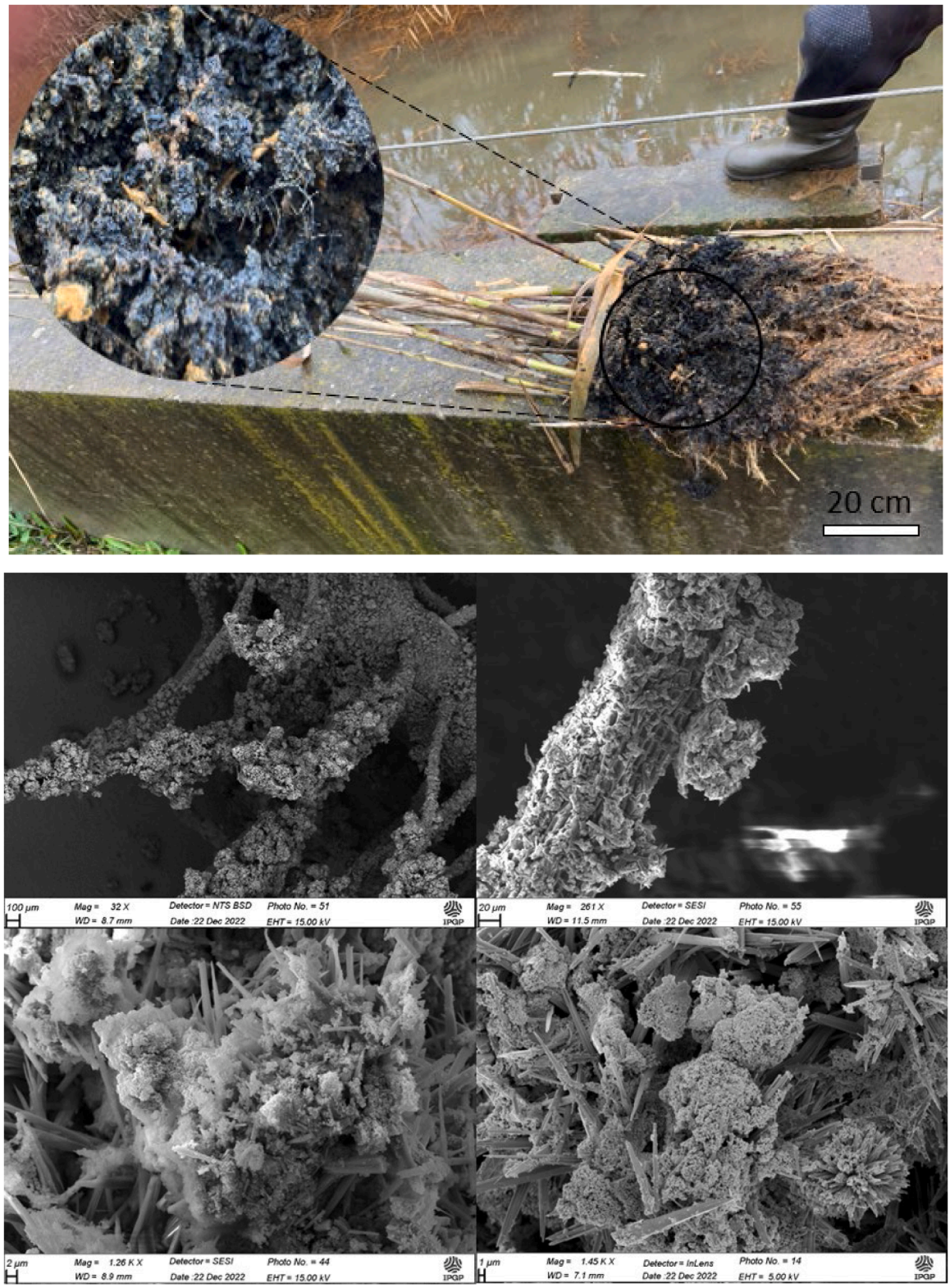

Fig. 5. Photograph of the Mn oxide rhizosphere plaque minerals sampled at the end of the third wetland (R). Scanning Electron Microscopy (SEM) images of the rhizosphere covered by plaque minerals: Top images show the large-scale structure of mineral accumulation on the rhizosphere, and bottom images provide a close-up view of mineral surface structure (left: SESI mode, and right: InLens mode).

3.4. The role of reeds in Mn removal

Reeds play a crucial role in wetland systems by acting as natural filters, trapping suspended particles, and promoting biofilm growth (Wolkersdorfer, 2022). They supply organic carbon, which enhances microbial activity that can facilitate Mn removal (Batty and Younger, 2002; Opitz et al., 2021; Wang et al., 2021). During our study, the second wetland was cured and mowed, resulting in the replacement of mature reeds with young shoots in early August. This event reduced the effectiveness of the treatment, as indicated by the decrease in removal rates of total Fe and dissolved Mn concentrations in the second wetland in August, most likely attributed to changes in hydraulic conditions (Fig. 2 and Table S3).

Beyond their role in physical filtration, reeds also influence Mn dynamics through rhizosphere-mediated processes. The formation of thick, dark Mn-rich precipitates in the form of mineral plates in the rhizosphere suggests prolonged Mn retention over time (Fig. 5). Poorly crystallised Mn oxides with a birnessite-type structure (Fig. 4) are present at both the rhizome-sediment interface and the rhizome-water interface, indicating that the rhizosphere can create localised conditions favourable to Mn oxidation (Faulwetter et al., 2009; Hansel et al., 2001). Elemental analyses suggest a preferential accumulation of Mn over Fe with a high Mn concentration of 21.54 g kg^{-1} (Table S5). Moreover, DET profiles revealed the absence of dissolved Mn and Fe in the pore waters of reed-rich areas (S2; Figure S6), in contrast to high concentrations in non-vegetated zones (S1; Figure S6). Despite anoxic conditions (Figure S7), these results suggest that the rhizosphere creates microscale redox gradients that favour Mn stabilising in rhizosphere but speciation changes may vary seasonally in response to changing geochemical and redox conditions.

Porous Mn oxide aggregates of 2 to 10 μm are observed on SEM images, resembling biogenic morphologies (Fig. 5) (Miyata et al., 2024). Oxygen release from roots, microbial colonisation and autocatalytic oxidation likely interact to sustain Mn accumulation (Hallberg and Johnson, 2005; Jacob et al., 2019). Temporal variation of reed physiological state could drive the root-associated phenomena, in particular in the third wetland. Oxygen release in roots is linked to photosynthesis, which is more active in summer than in winter, that might explain the higher Mn removal in June and the lower Mn removal in December (Fig. 2).

3.5. Microbial communities contributing to Mn removal

Microorganisms involved in the Mn redox cycle have been extensively studied across various systems, including passive mine water treatment, where their presence can significantly enhance Mn removal rates (Li et al., 2019; Santelli et al., 2010). At pH below 8, bacteria and fungi are recognised as the main catalysts of Mn oxidation, either through direct metabolic pathways (Yu and Leadbetter, 2020) or indirect mechanisms performed by microbial activity (Santelli et al., 2011; Tebo et al., 2005, 2004). In this study, we characterised the bacterial and fungal communities present in the passive treatment plant to identify taxa potentially involved in the identified Mn removal processes.

3.5.1. Bacterial community in mine water

In mine water, the bacterial community was investigated at the middle of the third wetland (W3; Fig. 1) and at the end of the third wetland (EW3; Fig. 1) with a bimonthly monitoring over one year. Although rarefaction curves suggest that some diversity may not have been fully captured (Figure S8), Chao1 and observed richness indexes suggest adequate sequencing depth for most samples (Table S7).

The dominant phyla are *Proteobacteria* (38-69 %), *Bacteroidota* (10-22 %), *Actinobacteria* (4-23 %), and *Cyanobacteria* (1-19 %) (Fig. 6A). The most abundant family is *Comamonadaceae*, representing around 24 % across all samples (Fig. 6B), commonly found in Mn-rich environments (Chaput et al., 2015; Zhang et al., 2002). Other families containing known Mn-oxidising bacteria included *Rhodobacteraceae, Flavobacteriaceae, Sphingomonadaceae,* and *Caulobacteraceae* (Hou et al., 2020; Santelli et al., 2010). Key genera included *Pseudorhodobacter, Rhodobacter, Flavobacterium, Polaromonas, Caulobacter, Hydrogenophaga, Asticcacaulis*, and *Leptothrix* (Marcus et al., 2017; Zhang et al., 2002). The calcite-forming bacteria, *Rheinheimera*, is also detected and may contribute to Mn carbonate precipitation (Fig. 6C) (Rivadeneyra et al., 2017).

Temporal monitoring in the third wetland revealed a stable bacterial community composition with similar taxa retrieved along the monitoring; however, their relative abundance varied (Fig. 6). The PCoA of the Bray-Curtis matrix confirmed a temporal variation in bacterial community structure (Fig. 7), with samples clustering according to sampling month. This finding indicates that bacterial community structure is primarily influenced by sampling time. Moreover, richness is lowest in December, coinciding with the lowest Mn removal efficiency, and highest in June, when Mn removal is the most effective (Tables S3 and S7). This pattern has been reported in other passive treatment plants, where environmental factors influencing bacterial metabolic activity rather than taxonomy profile drive Mn removal performance (Chaput et al., 2015).

3.5.2. Bacterial community in sediment and root zone

In sediment (S1, S2, and S3; Fig. 1) and rhizosphere mineral plaque (R; Fig. 1), a total of 126,470 16S rRNA sequences were obtained. Rarefaction curves did not quite reach a plateau, indicating that part of the bacterial diversity may not have been fully captured (Figure S8). Bacterial diversity is highest in the rhizosphere mineral plaque compared to the sediment samples (Table S7). Overall, bacterial richness and diversity were higher in solid samples than in water, suggesting that more complex processes and functionally diverse microbial communities are potentially involved in Mn cycling.

Across all solid samples, the most abundant phyla are *Proteobacteria* (15-35 %), *Bacteroidota* (8-19 %), and *Chloroflexi* (8-14 %) (Fig. 8). In sediments, *Proteobacteria* increased along the third wetland, from 15 % at S1 to 32 % at S3. The rhizosphere displays a similar taxonomic profile to S3, consistent with their spatial proximity and shared geochemical conditions.

At the family level, the community included taxa with potentially diverse metabolisms. Solid samples hosted a mixture of potential aerobic (*Comamonadaceae*) and anaerobic groups, including fermentative (*Spirochaetaceae*), sulphate-reducing (*Desulfosarcinaceae*), and metal-reducing (*Rhodocyclaceae*) taxa (Fig. 8). The determined bacteria can use Mn(II) from $MnCO_3$ as an electron donor or Mn(IV) from δ-MnO_2 as an electron acceptor, supporting redox cycling (Hatayama, 2020; Jia et al., 2023).

Several genera, including *Pedomicrobium, Pseudomonas, Rhodobacter, Hydrogenophaga* and *Rubrivivax,* emerged as potential Mn-oxidising bacteria in rhizosphere mineral plaque (Figure S9) (Marcus et al., 2017; Martínez-Ruiz et al., 2021). Other families, including *Rhodobacteraceae, Nitrosomonadaceae, Nitrospiraceae, Hyphomicrobiaceae, Xanthobacteraceae*, and *Anaerolineaceae*, likely contribute indirectly to Mn transformation through nitrogen cycling, redox interactions, or syntrophic associations (Tebo et al., 2005; Wang et al., 2021). The water-sediment-rhizosphere interfaces represent a complex system in which oxygen and organic compounds, produced by reeds or associated microorganisms, support both aerobic and anaerobic metabolic activities (Weiss et al., 2003).

3.5.3. Role of fungal communities in mine water

The fungal community in the third wetland (W3 and EW3) was characterised in April 2022, yielding a total of 240,700 ITS2 sequences. Rarefaction curves reached a plateau, indicating that fungal diversity was fully captured (Figure S8).

The dominant fungal phyla were *Ascomycota* and *Basidiomycota*, with a relative abundance of 64 % and 13 % on average, respectively

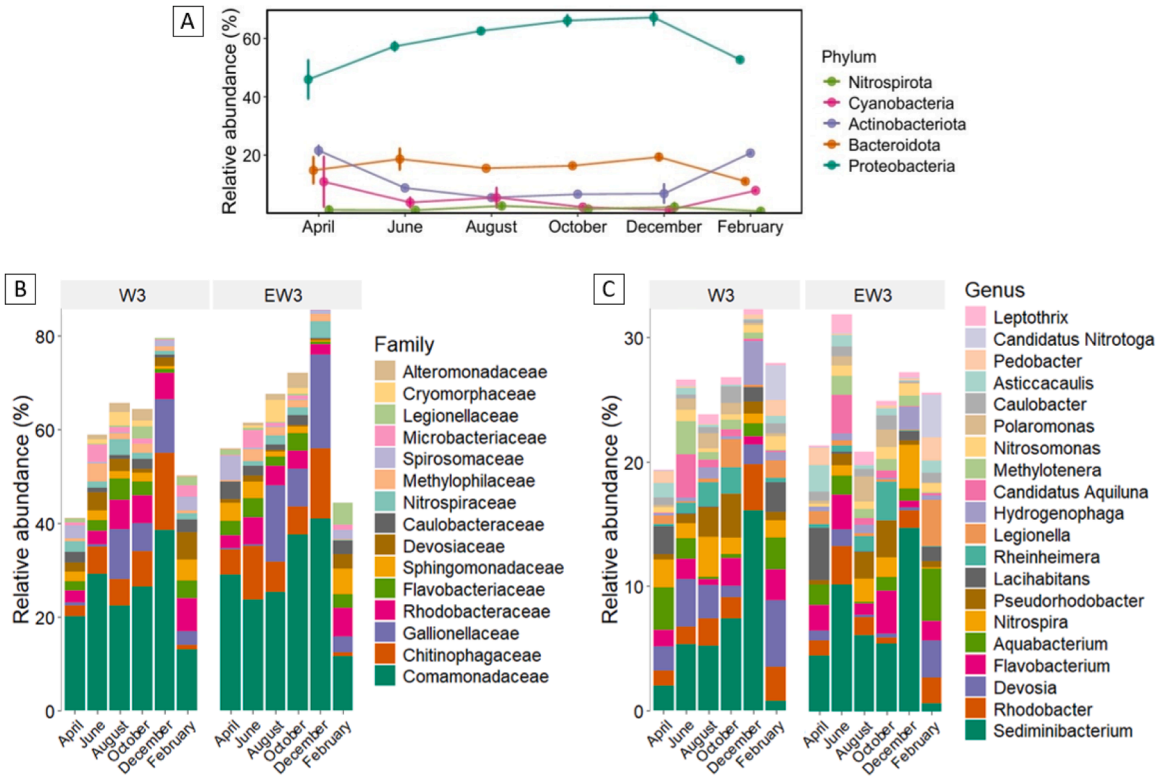

Fig. 6. Relative abundance of most abundant bacterial Amplicon Sequence Variants in water samples at different taxonomic levels: (A) phylum level (average across W3 and EW3 samples), (B) family level, and (C) genus level for each sampling location, including the middle of the third (W3) and end (EW3) of the third wetland, across all sampling campaigns.

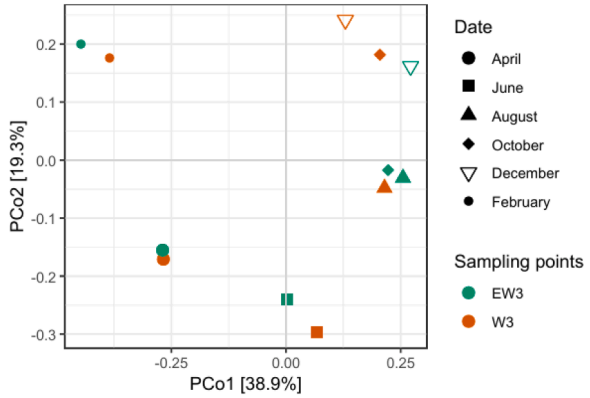

Fig. 7. Principal Coordinate Analysis (PCoA) based on Bray-Curtis distances of the relative abundance of the bacterial community retrieved from DNA from filtered water on Sterivex® including the samples from the middle of the third wetland (W3) and the end of the third wetland (EW3).

(Figure S10). A substantial portion of sequences (15-22 %) could not be taxonomically assigned at the phylum level. The dominant orders included *Sordariomycetes, Dothideomycetes* and *Tremellomycetes*, which have been observed in passive treatment systems for Mn removal (Chaput et al., 2015; Mariner et al., 2008).

Among the genera identified, sequences belonging to *Phoma* and *Fusarium* were detected (Figure S10). These genera are known as Mn(II)-oxidising fungi and have been observed in high abundance in coal mine drainage remediation systems (Santelli et al., 2010). The recurrent presence of these species in passive treatment plants suggest their potential role in Mn removal. However, the limited information available on Mn-oxidising fungal communities complicates interpretation and comparisons between fungal and bacterial contributions to Mn removal in natural samples (Chaput et al., 2015; Li et al., 2019).

3.6. *Environmental parameters correlated with bacterial communities in mine water*

The RDAs showed that environmental parameters explained 90.6 % and 78.3 % of the variance at the phylum and family levels, respectively, and revealed a monthly clustering of the bacterial community (Fig. 9). At the phylum level, the first axis, explaining 81.1 % of the variance, is mainly driven by Fe and alkalinity, and to a lesser extent, by temperature, calcium, Mn removal and dissolved Mn. These variables describe temporal shifts in dominant phyla including Proteobacteria and Actinobacteria, linked to changes of physicochemical conditions.

Most bacterial families are associated with months showing high Mn removal efficiency (April, June, August and February), whereas December, corresponding to the lowest Mn removal, is only dominated by *Comamonadaceae*. Although this family includes potential known Mn-oxidisers (Marcus et al., 2017; Tebo et al., 2005), it suggests that its abundance is not linked to Mn removal. *Cyanobacteria* correlate positively with dissolved Mn, suggesting that they likely do not drive Mn oxidation nor promote Mn carbonate precipitation (Benzerara et al., 2023; Jacob et al., 2022). *Cyanobacteria* abundance is likely driven by light availability, which may be influenced by shading from reeds in summer and reduced light in winter, making April and February optimal months for their growth (Fig. 6A).

Environmental variables such as temperature, total and dissolved Fe, alkalinity, dissolved Mn and ORP structured distinct bacterial clusters, highlighting the influence of physicochemical factors on bacterial community structure (Fig. 9). *Alteromonadaceae*, identified as the genus *Rheinheimera* and reported as a calcite-forming bacteria, is negatively correlated with alkalinity and dissolved Mn, consistent with a potential role in Mn carbonate precipitation (Hatayama, 2020). The presence of Gallionellaceae (family level) suggests a potential influence of microbial

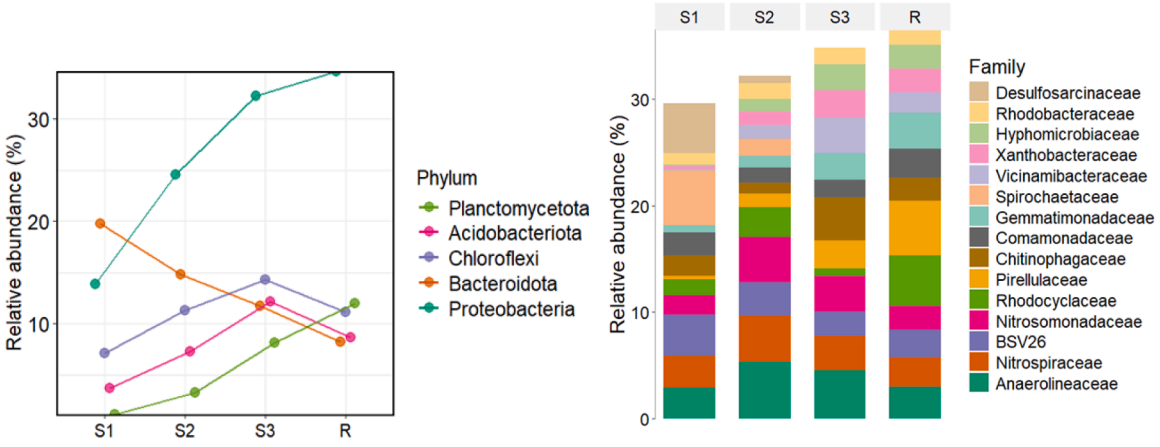

Fig. 8. Relative abundance of most abundant bacterial Amplicon Sequence Variants (ASVs) at different taxonomic levels identified in sediments and rhizosphere mineral plaque sampled in March 2023. The displayed data are the entrance of the third wetland (S1), the middle of the third wetland (S2), the end of the third wetland (S3), and the rhizosphere minerals plaque (R).

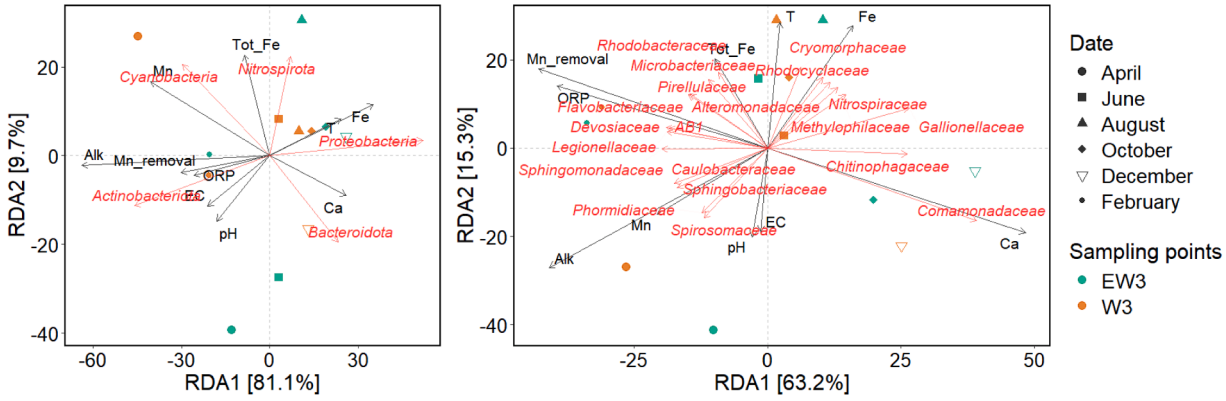

Fig. 9. Redundancy Analysis (RDA) depicting the relationship between environmental variables in water and the most abundant bacterial taxa at the phylum and family levels. Data included are the middle of the third wetland (W3) and the end of the third wetland (EW3). Red arrows indicate the bacterial communities, while black arrows represent environmental variables.

factors on the fate of Fe. At the phylum level, the RDA shows that alkalinity correlates with Mn removal, indicating its primary role in Mn attenuation at a broad ecological scale. However, the observed anti-correlation between dissolved Ca and Mn may indicate a competitive effect, potentially contributing to the slow kinetics of Mn-carbonate formation even if mine water is saturated regarding rhodochrosite in all wetland's units (Table S6).

Laboratory work has shown that microorganisms can catalyse Mn(II) oxidation or promote carbonate precipitation under favourable conditions, like the multicopper oxidase-mediated Mn oxidation (Tebo et al., 2004), the chemolithoautotrophic Mn oxidation (Yu and Leadbetter, 2020), or the calcifying bacteria facilitating Mn-carbonate formation (Rivadeneyra et al., 2017). In contrast, in full-scale constructed wetlands, abiotic factors appear to primary control Mn removal mechanisms, while bacterial taxa probably modulate or accelerate specific Mn removal processes only when the geochemical conditions are permissive.

4. Conclusion

While previous studies have mainly focused on Mn removal under controlled laboratory or pilot-scale conditions, this study provides new insights through a large-scale passive mine water treatment system operating under high alkalinity conditions. By integrating long-term performance monitoring with solid-phase speciation and microbial analyses, this work demonstrates that Mn removal is primarily governed by abiotic processes, notably carbonate precipitation in the water and Mn oxide formation in the rhizosphere of reeds. Comparison of three successive wetland units shows that effective Mn attenuation only occurs once specific geochemical and physical conditions are met, highlighting the critical role of seasonal changes and wetland configuration and area in controlling Mn removal on a large scale.

Two main elimination mechanisms have been identified. The precipitation of Mn carbonates ($MnCO_3$, rhodochrosite), favoured by the high carbonate content of the water, with dissolved calcium probably competing for carbonate precipitation. The formation of Mn oxides (δ-MnO_2, birnessite type) on the surface of reed roots. In the rhizosphere, the reactive surface of the roots probably promotes Mn removal by facilitating autocatalytic oxidation and creating microenvironments where biotic processes can contribute to Mn retention. Temporal variations in Mn removal efficiency appear to result from geochemical factors potentially combined with microbial processes, as well as climatic conditions such as light availability and temperature controlling reaction kinetics. Two main influencing factors were identified including elevated alkalinity, along with the presence of calcite-forming bacteria (such as *Rheinheimera*), and iron-suspended particles likely promoting Mn carbonate precipitation by providing nucleation sites. Although the overall composition of the bacterial community remained relatively stable, the microbial structure and environmental parameters showed temporal clustering consistent with seasonal trends. However, the

bimonthly sampling frequency does not allow for a fully resolved seasonal dynamic to be established.

From an engineering perspective, the third wetland exhibited the highest Mn area-normalised removal rates, suggesting that increasing the surface area of this wetland and optimising hydrological conditions may improve the overall efficiency of the treatment plant. Overall, this study provides large-scale evidence that Mn attenuation in highly alkaline mine waters is primarily controlled by abiotic processes, with microbial communities playing a secondary role. Future research should clarify the ecological roles of prokaryotic and fungal-mediated Mn removal processes through targeted studies, the role of Fe particles, and the relative contributions of abiotic and biotic processes.

Declaration of generative AI and AI-assisted technologies in the manuscript preparation process

During the preparation of this work the author(s) used ChatGPT in order to generate the code required for plotting and statistical analysis on R. After using this tool/service, the author(s) reviewed and edited the content as needed and take(s) full responsibility for the content of the published article.

CRediT authorship contribution statement

Charlotte Lafont: Writing – original draft, Visualization, Methodology, Investigation, Formal analysis. **Stéphane Vaxelaire:** Supervision, Resources, Investigation, Conceptualization. **Alexandre Gelabert:** Writing – review & editing, Resources, Investigation. **Catherine Joulian:** Writing – review & editing, Investigation, Conceptualization. **Hugues Thouin:** Writing – review & editing, Formal analysis. **Frédéric Duré:** Investigation. **Mickael Charron:** Investigation. **Josselin Gorny:** Writing – review & editing, Resources, Investigation. **Delphine Vantelon:** Writing – review & editing, Resources, Investigation, Formal analysis. **Fabienne Battaglia-Brunet:** Writing – review & editing, Supervision, Investigation, Funding acquisition, Conceptualization. **Éric D. van Hullebusch:** Writing – review & editing, Supervision, Investigation, Funding acquisition, Conceptualization.

Declaration of competing interest

The authors declare that they have no known competing financial interests or personal relationships that could have appeared to influence the work reported in this paper.

Acknowledgements

We thank Mathilde Zebracki from ASNR for providing the equipment for field measurements and guidance in teaching me how to use it effectively. We acknowledge SOLEIL for the provision of synchrotron radiation facilities (project numbers 20221221 and 20231954), and we would like to thank Delphine Vantelon and her team for assistance in using LUCIA beamline. This work was supported by the Department for Mine Safety and Risk Prevention (DPSM) of the French Geological Survey (BRGM). Some of this work was also supported by the IPGP multidisciplinary program PARI and the Paris–IdF region SESAME [Grant no. 12015908]. The graphical abstract was created in BioRender. Lafont, C. (2025) https://BioRender.com/lc1rd15.

Supplementary materials

Supplementary material associated with this article can be found, in the online version, at doi:10.1016/j.watres.2026.125539.

Data availability

Data will be made available on request.

References

Bamforth, S.M., Manning, D.A., Singleton, I., Younger, P.L., Johnson, K.L., 2006. Manganese removal from mine waters–investigating the occurrence and importance of manganese carbonates. Appl. Geochem. 21, 1274–1287. https://doi.org/10.1016/j.apgeochem.2006.06.004.

Bamforth, S.M., Satterley, C., 2022. Evaluating manganese in mine water in UK coal authority mine water schemes. In: Proc. IMWA 2022 Reconnect Conf, pp. 7–13.

Batty, L.C., Younger, P.L., 2002. Critical role of macrophytes in achieving low iron concentrations in mine water treatment wetlands. Environ. Sci. Technol. 36, 3997–4002. https://doi.org/10.1021/es020033. +.

Benzerara, K., Elmaleh, A., Ciobanu, M., De Wever, A., Bertolino, P., Iniesto, M., Jézéquel, D., López-García, P., Menguy, N., Muller, E., 2023. Biomineralization of amorphous Fe-, Mn-and Si-rich mineral phases by cyanobacteria under oxic and alkaline conditions. Biogeosciences 20, 4183–4195. https://doi.org/10.5194/bg-20-4183-2023.

Chaput, D.L., Hansel, C.M., Burgos, W.D., Santelli, C.M., 2015. Profiling microbial communities in manganese remediation systems treating coal mine drainage. Appl. Environ. Microbiol. 81, 2189–2198.

Davies, S.H., Morgan, J.J., 1989. Manganese (II) oxidation kinetics on metal oxide surfaces. J. Colloid Interface Sci. 129, 63–77. https://doi.org/10.1016/0021-9797(89)90416-5.

Diem, D., Stumm, W., 1984. Is dissolved Mn2+ being oxidized by O2 in absence of Mn-bacteria or surface catalysts? Geochim. Cosmochim. Acta 48, 1571–1573. https://doi.org/10.1016/0016-7037(84)90413-7.

Faulwetter, J.L., Gagnon, V., Sundberg, C., Chazarenc, F., Burr, M.D., Brisson, J., Camper, A.K., Stein, O.R., 2009. Microbial processes influencing performance of treatment wetlands: a review. Ecol. Eng. 35, 987–1004. https://doi.org/10.1016/j.ecoleng.2008.12.030.

Hallberg, K.B., Johnson, D.B., 2005. Biological manganese removal from acid mine drainage in constructed wetlands and prototype bioreactors. Sci. Total Environ., Bioremed. Acid Mine Drainage 338, 115–124. https://doi.org/10.1016/j.scitotenv.2004.09.011.

Hansel, C.M., Fendorf, S., Sutton, S., Newville, M., 2001. Characterization of Fe plaque and associated metals on the roots of mine-waste impacted aquatic plants. Environ. Sci. Technol. 35, 3863–3868. https://doi.org/10.1021/es0105459.

Hatayama, K., 2020. Manganese carbonate precipitation induced by calcite-forming bacteria. Geomicrobiol. J. 37, 603–609. https://doi.org/10.1080/01490451.2020.1743391.

Hedin, R.S., 2008. Iron removal by a passive system treating alkaline coal mine drainage. Mine Water Environ. 27, 200–209. https://doi.org/10.1007/s10230-008-0041-9.

Hedin, R.S., Nairn, R.W., Kleinmann, R.L., 1994. Passive treatment of coal mine drainage. US Department of the Interior, Bureau of Mines.

Hou, D., Zhang, P., Wei, D., Zhang, J., Yan, B., Cao, L., Zhou, Y., Luo, L., 2020. Simultaneous removal of iron and manganese from acid mine drainage by acclimated bacteria. J. Hazard. Mater. 396, 122631. https://doi.org/10.1016/j.jhazmat.2020.122631.

Jacob, J., Joulian, C., Battaglia-Brunet, F., 2022. Start-up and performance of a full scale passive system in-cluding biofilters for the treatment of Fe, as and Mn in a neutral mine drainage. Water 14, 1963. https://doi.org/10.3390/w14121963.

Jacob, J., Raignault, I., Battaglia-Brunet, F., Mailhan-Muxi, C., Engevin, J., Djemil, M., 2019. Biological manganese removal from mine drainage in a fixed bed bioreactor at pilot scale. Mine Closure, 2019. https://brgm.hal.science/hal-02146705v1.

Jia, L., Zhou, Q., Li, Y., Wu, W., 2023. Application of manganese oxides in wastewater treatment: Biogeochemical Mn cycling driven by bacteria. Chemosphere 336, 139219. https://doi.org/10.1016/j.chemosphere.2023.139219.

Kruse, N.A.S., Younger, P.L., 2009. Sinks of iron and manganese in underground coal mine workings. Environ. Geol. 57, 1893–1899. https://doi.org/10.1007/s00254-008-1478-7.

Lan, S., Qin, Z., Wang, X., Yan, Y., Tang, Y., Feng, X., Zhang, Q., 2021. Kinetics of Mn (II) adsorption and catalytic oxidation on the surface of ferrihydrite. Sci. Total Environ. 791, 148225. https://doi.org/10.1016/j.scitotenv.2021.148225.

Lesley, B., Daniel, H., Paul, Y., 2008. Iron and manganese removal in wetland treatment systems: rates, processes and implications for management. Sci. Total Environ. 394, 1–8. https://doi.org/10.1016/j.scitotenv.2008.01.002.

Li, Y., Xu, Z., Ma, H., S Hursthouse, A., 2019. Removal of manganese (II) from acid mine wastewater: a review of the challenges and opportunities with special emphasis on Mn-oxidizing bacteria and microalgae. Water 11, 2493. https://doi.org/10.3390/w11122493.

Liu, J., Chen, Q., Yang, Y., Wei, H., Laipan, M., Zhu, R., He, H., Hochella Jr, M.F., 2022. Coupled redox cycling of Fe and Mn in the environment: the complex interplay of solution species with Fe-and Mn-(oxyhydr) oxide crystallization and transformation. Earth-Sci. Rev. 232, 104105. https://doi.org/10.1016/j.earscirev.2022.104105.

Luan, F., Burgos, W.D., 2019. Effects of solid-phase organic carbon and hydraulic residence time on manganese(II) removal in a passive coal mine drainage treatment system. Mine Water Environ. 38, 130–135. https://doi.org/10.1007/s10230-018-0548-7.

Marcus, D.N., Pinto, A., Anantharaman, K., Ruberg, S.A., Kramer, E.L., Raskin, L., Dick, G.J., 2017. Diverse manganese (II)-oxidizing bacteria are prevalent in drinking water systems. Environ. Microbiol. Rep. 9, 120–128. https://doi.org/10.1111/1758-2229.12508.

Mariner, R., Johnson, D.B., Hallberg, K.B., 2008. Characterisation of an attenuation system for the remediation of Mn (II) contaminated waters. Hydrometallurgy 94, 100–104.

Martínez-Ruiz, E.B., Cooper, M., Barrero-Canosa, J., Haryono, M.A., Bessarab, I., Williams, R.B., Szewzyk, U., 2021. Genome analysis of Pseudomonas sp. OF001 and

Rubrivivax sp. A210 suggests multicopper oxidases catalyze manganese oxidation required for cylindrospermopsin transformation. BMC Genomics 22, 464. https://doi.org/10.1186/s12864-021-07766-0.

Miyata, N., Suganuma, R., Sunouchi, K., Okano, K., Fuchida, S., Watanabe, M., Fujibayashi, M., Sato, Y., Tokoro, C., 2024. Biological Mn (II) oxidation under organic substrate-limited conditions and its application in mine drainage remediation. Biochem. Eng. J. 203, 109187. https://doi.org/10.1016/j.bej.2023.109187.

Moorhouse-Parry, A.M., Satterley, C.J., 2023. Assessment of manganese removal in passive systems based on operational data and experience of treating net-alkaline coal mine waters in the UK. In: Proc. IMWA 2023 Future Conf, pp. 351–357.

Morgan, J.J., 2005. Kinetics of reaction between O2 and Mn (II) species in aqueous solutions. Geochim. Cosmochim. Acta 69, 35–48. https://doi.org/10.1016/j.gca.2004.06.013.

Neculita, C.M., Rosa, E., 2019. A review of the implications and challenges of manganese removal from mine drainage. Chemosphere 214, 491–510. https://doi.org/10.1016/j.chemosphere.2018.09.106.

Oliva, J., De Pablo, J., Cortina, J.-L., Cama, J., Ayora, C., 2010. The use of Apatite II™ to remove divalent metal ions zinc(II), lead(II), manganese(II) and iron(II) from water in passive treatment systems: column experiments. J. Hazard. Mater. 184, 364–374. https://doi.org/10.1016/j.jhazmat.2010.08.045.

Opitz, J., Alte, M., Bauer, M., Peiffer, S., 2021. The role of macrophytes in constructed surface-flow wetlands for mine water treatment: a review. Mine Water Environ. 40, 587–605. https://doi.org/10.1007/s10230-021-00779-x.

Ray, S., Dey, K., 2020. Coal mine water drainage: the current status and challenges. J. Inst. Eng. India Ser. D 101, 165–172. https://doi.org/10.1007/s40033-020-00222-5.

Rivadeneyra, A., Gonzalez-Martinez, A., Portela, G.R., Martin-Ramos, D.J., Gonzalez-Lopez, J., Rivadeneyra, M.A., 2017. Biomineralisation of carbonate and sulphate by the halophilic bacterium Halomonas maura at different manganese concentrations. Extremophiles 21, 1049–1056. https://doi.org/10.1007/s00792-017-0965-8.

Santelli, C.M., Pfister, D.H., Lazarus, D., Sun, L., Burgos, W.D., Hansel, C.M., 2010. Promotion of Mn (II) oxidation and remediation of coal mine drainage in passive treatment systems by diverse fungal and bacterial communities. Appl. Environ. Microbiol. 76, 4871–4875. https://doi.org/10.1128/aem.03029-09.

Santelli, C.M., Webb, S.M., Dohnalkova, A.C., Hansel, C.M., 2011. Diversity of Mn oxides produced by Mn (II)-oxidizing fungi. Geochim. Cosmochim. Acta 75, 2762–2776. https://doi.org/10.1016/j.gca.2011.02.022.

Schaefer, M.V., Plaganas, M., Abernathy, M.J., Aiken, M.L., Garniwan, A., Lee, I., Ying, S. C., 2020. Manganese, arsenic, and carbonate interactions in model oxic groundwater systems. Environ. Sci. Technol. 54, 10621–10629. https://doi.org/10.1021/acs.est.0c02084.

Skousen, J., Zipper, C.E., Rose, A., Ziemkiewicz, P.F., Nairn, R., McDonald, L.M., Kleinmann, R.L., 2017. Review of passive systems for acid mine drainage treatment. Mine Water Environ. 36, 133–153. https://doi.org/10.1007/s10230-016-0417-1.

Tebo, B.M., Bargar, J.R., Clement, B.G., Dick, G.J., Murray, K.J., Parker, D., Verity, R., Webb, S.M., 2004. Biogenic manganese oxides: properties and mechanisms of formation. Annu. Rev. Earth Planet Sci. 32, 287–328. https://doi.org/10.1146/annurev.earth.32.101802.120213.

Tebo, B.M., Clement, B.G., Dick, G.J., 2007. Biotransformations of manganese. Man. Environ. Microbiol. 1223–1238. https://doi.org/10.1128/9781555815882.ch100.

Tebo, B.M., Johnson, H.A., McCarthy, J.K., Templeton, A.S., 2005. Geomicrobiology of manganese (II) oxidation. TRENDS Microbiol. 13, 421–428. https://doi.org/10.1016/j.tim.2005.07.009.

Tum, S., Katayama, T., Miyata, N., Watanabe, M., Hashimoto, Y., Nishikata, M., Yasutaka, T., 2024. Geochemical insights and model optimisation for pilot-scale passive treatment of manganese and zinc in a legacy mine in Japan. Heliyon 10, e40363. https://doi.org/10.1016/j.heliyon.2024.e40363.

Wang, D., Lin, H., Ma, Q., Bai, Y., Qu, J., 2021. Manganese oxides in Phragmites rhizosphere accelerates ammonia oxidation in constructed wetlands. Water Res. 205, 117688. https://doi.org/10.1016/j.watres.2021.117688.

Weiss, J.V., Emerson, D., Backer, S.M., Megonigal, J.P., 2003. Enumeration of Fe (II)-oxidizing and Fe (III)-reducing bacteria in the root zone of wetland plants: implications for a rhizosphere iron cycle. Biogeochemistry 64, 77–96. https://doi.org/10.1023/A:1024953027726.

Wolkersdorfer, C., 2022. Mine Water Treatment – Active and Passive Methods. Springer Nature.

World Health Organization, 2004. Manganese in drinking-water: background document for development of WHO guidelines for drinking-water quality, in: manganese in drinking-water: background document for development of WHO guidelines for drinking-water quality.

Younger, P.L., Banwart, S.A., Hedin, R.S., Younger, P.L., Banwart, S.A., Hedin, R.S., 2002. Passive treatment of polluted mine waters. Mine Water Hydrol. Pollut. Remediat. 311–396. https://doi.org/10.1007/978-94-010-0610-1_5.

Younger, P.L., Wolkersdorfer, C., 2004. Mining impacts on the fresh water environment: technical and managerial guidelines for catchment scale management. Mine Water Environ. 23, s2–s80. https://doi.org/10.1007/s10230-004-0028-0.

Yu, H., Leadbetter, J.R., 2020. Bacterial chemolithoautotrophy via manganese oxidation. Nature 583, 453–458. https://doi.org/10.1038/s41586-020-2468-5.

Zeng, Z., Tice, M.M., 2014. Promotion and nucleation of carbonate precipitation during microbial iron reduction. Geobiology 12, 362–371. https://doi.org/10.1111/gbi.12090.

Zhang, J., Lion, L.W., Nelson, Y.M., Shuler, M.L., Ghiorse, W.C., 2002. Kinetics of Mn (II) oxidation by Leptothrix discophora SS1. Geochim. Cosmochim. Acta 66, 773–781. https://doi.org/10.1016/S0016-7037(01)00808-0.